Advance Researches in Civil Engineering
ISSN: 2645-7229, Vol.4, No.4, pages: 1-15

Comparison of Fragility Assessment Isolated Structures Mounted on TCFP Bearings Subjected to Near Field and Far Field Earthquakes

Nesa Hazrati [1*], Faramarz Khoshnoudian [2]

[1] M.Sc. student of structural Engineering, Faculty of Civil Engineering, Amirkabir University of Technology, Tehran, Iran*

(nhazrati@aut.ac.ir)

[2] Professor, Faculty of Civil Engineering, Amirkabir University of Technology, Tehran, Iran

(Date of received: 24/05/2022, Date of accepted: 14/10/2022)

ABSTRACT

In recent years, isolated systems are noted for preserving structures against harmful effects of earthquakes. Across all types of friction isolators, the latest one, triple concave friction pendulum, is transcending for its hardening behavior in high risk states. Isolated systems dissipate energy of earthquakes by increasing period and damping. In this paper, the behavior of structures (3, 6, and 9 stories) mounted on TCFP subjected to near-field and far-field earthquakes are studied using fragility curves concept. Results indicate by increasing the effective period of TCFP decreases the median acceleration of collapse damage state (Sa-50% collapse). For better understanding the behavior of TCFP isolators with different effective periods, collapse margin ratio is also used, that demonstrates isolator with higher period reduces collapse risk. Comparing Sa-50% collapse in structure subjected to near-field and far-field earthquakes shows that the structure subjected to near field earthquake is less than the far field one.

Keywords:

Far field earthquakes, Near field earthquakes, Seismic isolator, TCFP isolator, IDA, Fragility curve.

1. Introduction

Engineers always attempt to mitigate damages and harmful effects of earthquakes on structures. Among various methods to dissipate the energy of earthquakes, base isolating is a favorable method for protection of structures from earthquakes. Main parameters that preserve the isolated structures are flexibility and the inherent energy dissipation system in base isolations. The isolators are mainly categorized as elastomeric and frictional ones. Three types of frictional bearings are introduced as single friction pendulum (SFP) which is the most well-known frictional bearing [1-4] double concave friction pendulum (DCFP) [5-9] and triple concave friction pendulum (TCFP) bearings that are two improved kinds of frictional bearings. The latest and third generation of frictional isolators is triple concave friction pendulum (TCFP). Fenz and Constantinou [10] reported the mathematical model and formulation of TCFP. They introduce a series model that consists of three FPS isolators connected in series to obtain the behavior of TCFP isolators. Fadi and Constantinou [11] used a simplified method of analysis with a SDOF system for a structure isolated with TCFP having linear stiffness and viscous damping. They concluded that this simplification underestimated the peak velocity and it had an acceptable isolator displacement. Morgan and Mahin [12] studied the behavior of TCFP isolators and Bi-Linear isolators, and indicated the reliable performance of TCFP isolators against Bi-Linear behavior devices. Becker and Mahin studied and examined bi-directional behavior TCFP isolators [13]. Loghman and Khoshnoudian [14] investigated buildings mounted on FPS, DCFP, and TCFP. Results showed that decreasing effective isolation damping and increasing effective period of isolation improved the seismic behavior of TCFP in comparison with other isolators. Loghman et al. [2015.a] [15] studied the effect of vertical component on seismic responses of TCFP base-isolated structures. Loghman et al. [2015.b] [16] investigated the effects of considering rotational components of earthquake on seismic responses of buildings mounted on TCFP base-isolation that showed increase in some seismic responses. Khoshnoudian and Fallahian [17] investigated the responses of torsionally base-isolated structure supported on TCFP. Tajammolian et al. [18] investigated the effects of mass asymmetric structures mounted on TCFP base-isolation subjected to near-fault ground motion. Becker et al. [19] conducted different tests on a TFP-isolated structure subjected to extreme earthquake loading considering experimental and numerical model in order to investigate the behavior of TFP-isolated structures. Xu et al. [20] analyzed a 33-story RC building in China located on medium stiff soil and investigated optimal design for TCFP bearings parameters. By regarding the floor acceleration, hysteresis loop responses, and story drift, triple friction pendulum bearings have more reliable behavior. Dao et al. [21] studied the prediction of global responses of a tested buildings mounted on TFP bearings, evaluating the ability of simplified computational models. They used two shear frame models and a single story model for simplified superstructure models. In this study three different story buildings (3, 6, and 9) are considered, which each of them mounted on three TCFP base-isolation with different periods (3, 4, and 5 second). Each model subjected to near field as well as far field earthquakes and they are analyzed with incremental dynamic analysis (IDA). The seismic performance of structures are studied through the damage states introduced by HAZUS [22], so that fragility curves are obtained and structures are compared with collapse margin ratio (CMR). Finally, fragility curves of same structures subjected to far field and near field earthquakes are compared.

Advance Researches in Civil Engineering
ISSN: 2645-7229, Vol.4, No.4, pages: 1-15

2. Seismic behavior of TCFP isolator

The latest type of friction isolator is triple concave friction pendulum (TCFP). The behavior of TCFP bearing is more complicated than the other friction isolators because it has more sliding surfaces. A TCFP isolator consists of four concave plates that are separated by an articulated slider in the middle of them [Constantinou et al.,] [23]. Figure 1. By thoroughly adjustment of plates' radii and friction coefficients, a 5-regime backbone curve is obtained shown in Figure 2. The main advantage of TCFP isolator in comparison to other friction isolators (FPS and DCFP) with bilinear and tri-linear behaviors is the hardening regimes at the end of its backbone curve (in phases IV and V). A comprehensive study was done for formulating the force-displacement relation for TCFP bearings by Fenz and Constantinou [24].

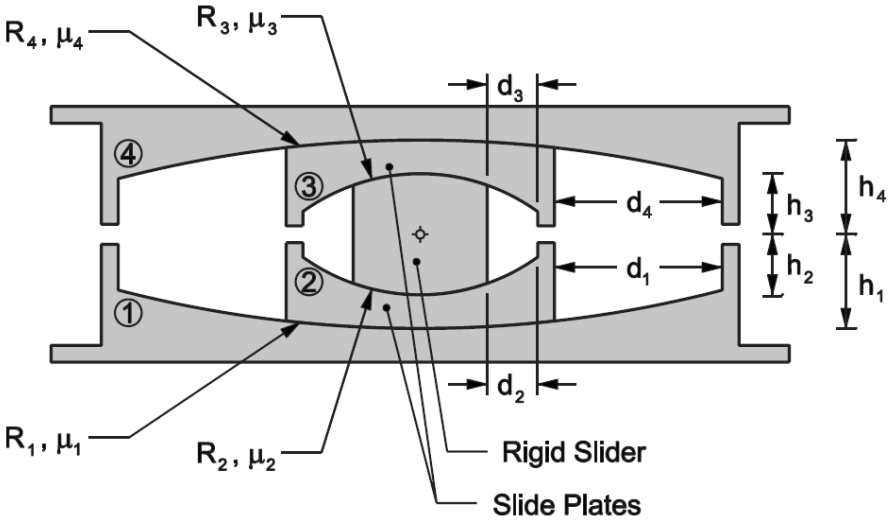

Figure 1. TCFP isolator [23].

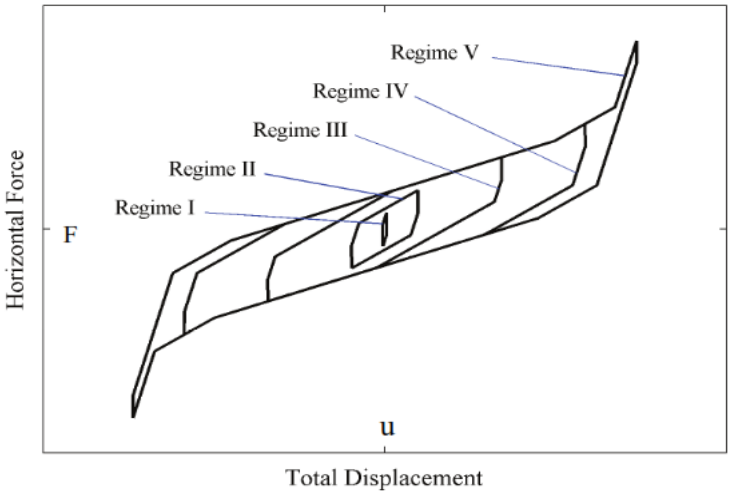

Figure 2. Backbone curve of TCFP [24].

3. Seismic behavior of TCFP isolator

One of the most important aspects of earthquake engineering based on the performance is the estimation of a structure performance subjected to seismic loads. The method that is presented for this approach is called incremental dynamic analysis (IDA). IDA is a method of analysis which considers inherent randomness of earthquake records. In this method a record is scaled in multiple analyses to represent a great range of ground motion intensities. FEMA P-695 [25] recommendation suggest the IDA procedure for anticipating the structural collapse margins.The IDA method is performed based on the hunt & fill algorithm proposed by Vamvatsikos and Cornell [26]. In this paper, for each far field and near field earthquakes, 15 records are selected from Pacific Earthquake Engineering NGA Database (PEER NGA) according to FEMA P-695 [25].

4. Fragility curves

The HAZUS damage assessment methodology FEMAI/NIBS (earthquake loss estimate methodology) is one of the most recent recommendations for estimating damage to a wide range of different structures [HAZUS-MH 2.1] [22]. Fragility functions define the conditional probability of attaining or exceeding a specified damage state. Four damage states are defined in this recommendation: Slight, Moderate, and Extensive or complete, and Collapse as subset of complete structural damage. Fragility curves for the four damage states used in the FEMA/NIBS methodology is illustrated in Figure 3 [HAZUS-MH 2.1] [22]. In this paper, damage state 4 is considered to prevent structures from collapse.

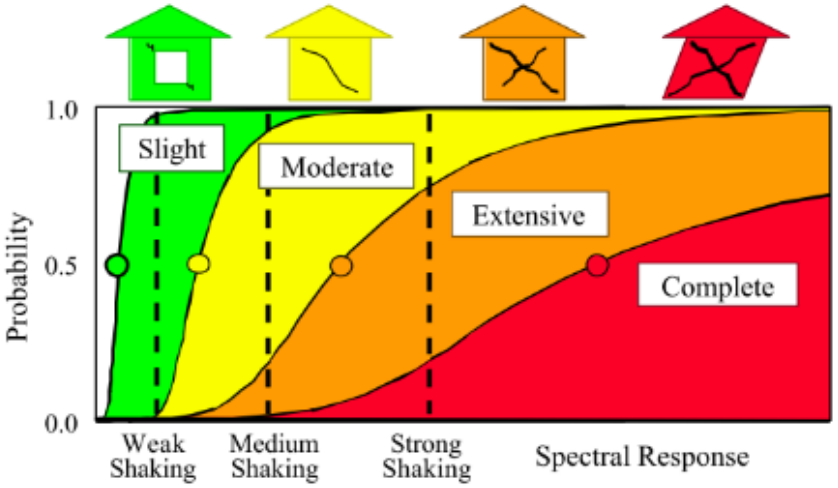

Figure 3. Fragility curves for different damage states [22].

Fragility curves can be defined as the probability that a structure exceeds a damage state. Zhan and Huo [27] offered an efficient way to select optimum isolation design parameters by evaluating effectiveness and optimum design of isolation devices for highway bridges under the fragility function. Tavares et al. [28] evaluated a fragility analysis of a 30 years old bridge with elastomeric bearings in Quebec, Canada. A series of 180 synthetic ground motion compatible with eastern Canada were used. They concluded that the column vulnerability governed fragility curves. Han et al. [29] studied a building before and after retrofitting with LRB base-isolation. They demonstrated that the effectiveness of base isolation in reducing seismic risk for higher damage level. Zhou et al. [30] investigated a tall reinforced concrete chimney in china considering fragility curves. The results revealed that the RC chimney had considerable ductility and was capable to withstand strong

earthquakes having structural damages without failure. Phan et al. [31] by using fragility function studied the effect of seismic concave sliding bearing on the vulnerability mitigation of liquefied gas tanks. Castaldo et al. [32] had similar research for friction based isolation systems using fragility function. They used reliability terms for analyzing the response of elastic structural systems equipped with friction pendulum isolator. Castaldo et al. [33] studied elastic RC structural systems mounted on FPS with different seismic levels and soil conditions by using fragility curves. As the previous background in the field of fragility assessment of TCFP isolated structures under near filed earthquakes reveals, there is a lack of knowledge for the comparison of fragility assessment TCFP isolated structures subjected to near field and far field earthquakes. It is necessary to elucidate this subject that has not been addressed so far. In this paper, for having a better comparison of fragility curves, the median acceleration of collapse state (Sa-50% collapse) is used. Sa-50% means the intensity measure with 50% of probability of occurrence. While structures with different periods are considered, collapse margin ratio (CMR) is used which is defined in FEMA P-695. According to FEMA-P695, CMR is defined as [25]:

$$CMR= \hat{S}_{CT}/S_{MT} \quad (1)$$

Where $\hat{S}_{CT}$ and S_{MT} represent respectively the ratio of the median 5%-damped spectral acceleration of the collapse level ground motions and the 5%-damped spectral acceleration of the MCE ground motions.

5. Design and modeling

5.1. Superstructure

In this research, structures are assumed to be in square plans. To create a reasonable range, 3 superstructures in 3, 6, and 9 stories with 3 bays in width and length are considered. Height of each story and length of each bay are assumed to be 3.33m and 5m respectively. Live and dead load assumed 4 and 8 KN/m^2 according to ASCE7-10 [34]. Superstructures have steel special moment frames which are designed according to AISC Specifications for Structural Steel Buildings (AISC60-10) using LRFD method [35]. And checked with minimum requirements of AISC 341-10 (Seismic Provisions for Structural Steel Buildings) [36]. Box-type sections are assumed for columns and standard I-shape profiles are selected for beams. Designed frame sections are illustrated in Figure 4.

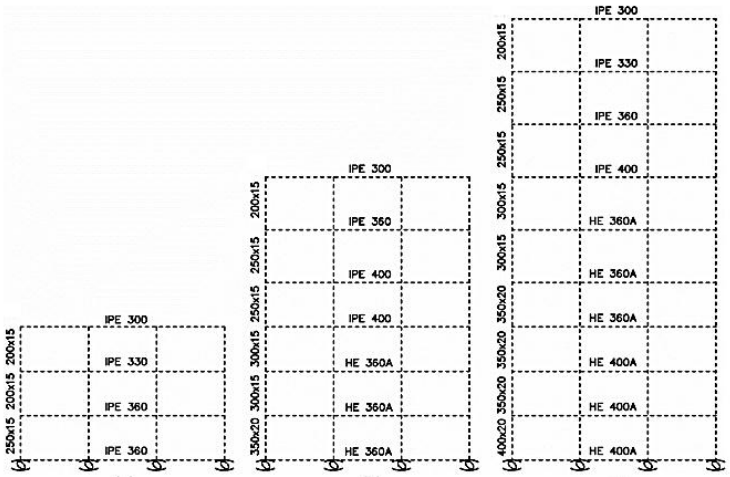

Figure 4. Designed sections.

The representative plan, which is an unconventional steel structure, is assumed in order to simulate rigid diaphragms of the floors so this simplification help us with lots of analyses during the IDA. OpenSees software (Open System for Earthquake Engineering Simulation) [37] is used for finite element analysis. This software is often used for nonlinear, reliability and sensitive analyses. Nonlinear sections of columns and beams are modeled with fiber element. In the sections of the wide plasticity fiber, the cross-sectional area is classified into types of meshes, and by defining different points of the cross-section, the stress-strain relations and materials related to each one are defined [38]. One of the vital advantages of fiber is considering the interaction of axial force and bending moment.

5.2. Isolator

Two important parameters for designing isolators to estimate the overall behavior of them are effective period (T_{eff}) and effectives damping (ζ_{eff}). In constantinou and Fadi [11], Beker and Mahin [13] researches, these two parameters are used for isolator designs. These parameters can be expressed by the following equations:

$$T_{eff} = 2\pi\sqrt{\frac{W}{K_{eff}\, g}} \tag{2}$$

$$\xi_{eff} = \frac{1}{2\pi}\left[\frac{E_{loop}}{K_{eff}D^2}\right] \tag{3}$$

In these equations W is the weight of structure ,k_{eff} presents the effective linear stiffness of isolator, E_{loop} stands for the energy dissipated in each cycle of the hysteresis loop and D denotes the target displacement of the isolator at the end of sliding regime IV that can be computed by the formulas introduced in ASCE 7-10 [34]. Maximum Considered Earthquake (MCE) hazard level is proposed for the design of TCFP isolators. E_{loop} and k_{eff} can be obtained from following equations. By having these two parameters effective period and effective damping can be calculated.

$$K_{eff} = \frac{F_{dr4}}{U_{dr4}} \tag{4}$$

$$\begin{aligned} E_{loop} = 4\left(\mu_1 + \frac{d_1}{R_{eff1}} - \frac{1}{R_{eff1}+R_{eff2}}u_{dr1}\right)u_{dr4}W \\ - 4\left(\frac{1}{R_{eff1}+R_{eff4}} - \frac{1}{R_{eff1}+R_{eff2}}\right)u_{dr1}^2 W \\ - 4\left(\frac{1}{R_{eff1}+R_{eff2}} - \frac{1}{R_{eff1}+R_{eff4}}\right)u^{**^2}W \\ - 4\left(\frac{1}{R_{eff2}+R_{eff3}} - \frac{1}{R_{eff1}+R_{eff2}}\right)u^{*^2}W \end{aligned} \tag{5}$$

Where u_{dr4} depends on the previous sliding regime displacements and u*, u** and u_{dr1} are the isolator displacement at the end of sliding regimes I, II, and III, respectively. R_{eff1} to R_{eff4} are effective radii for slide plates of 1 to 4 and F_{dr4} stands for the horizontal force. Figure 5.

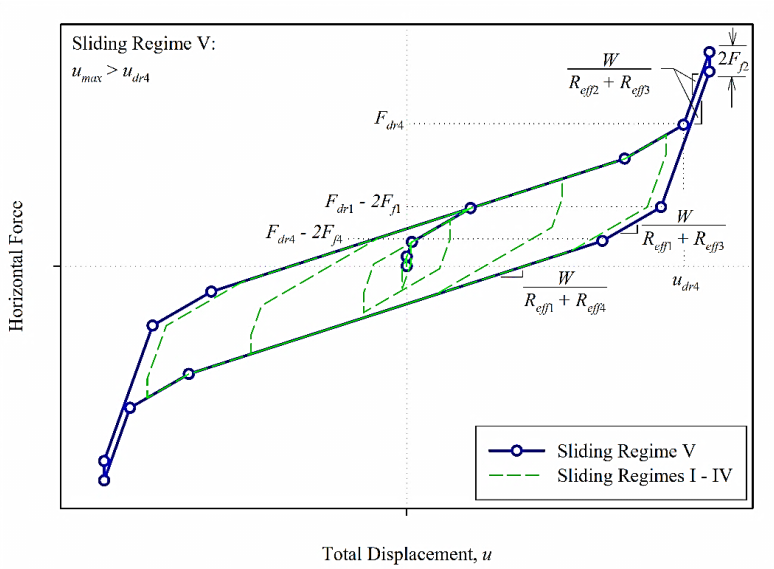

Figure 5. Force-displacement curve of TCFP.

In this paper, to cover a wide range of effective periods of isolators' 3 different isolators with T_{eff} 3, 4, and 5 second are assumed. Effective damping for designed isolators is selected as 15%. Designed isolators with different periods and their properties are presented in Table 1.

Table 1. Property of isolators.

		Displacement Capacity (m)		R_{eff} (m)		μ		
T_{eff} (sec)	$_{eff}$ (%)ζ	d_1=d_4	d_2=d_3	R_{eff1} = R_{eff4}	R_{eff2} = R_{eff3}	$_3\mu_2$ = μ	$_1\mu$	$_4\mu$
3	15	0.45	0.05	2.0	0.3	0.05	0.115	0.2
4	15	0.45	0.05	3.5	0.3	0.02	0.06	0.11
5	15	0.45	0.05	5.5	0.45	0.02	0.04	0.07

6. Results

6.1. Reference example

Firstly, IDA was applied to each types of models and the fragility curves were extracted. Secondly, the comparison of the median acceleration collapse of different models were considered. For example one of the IDA diagram is plotted in Figure 6. Θmax in Figure 6 stands for maximum inter story drift.

Advance Researches in Civil Engineering
ISSN: 2645-7229, Vol.4, No.4, pages: 1-15

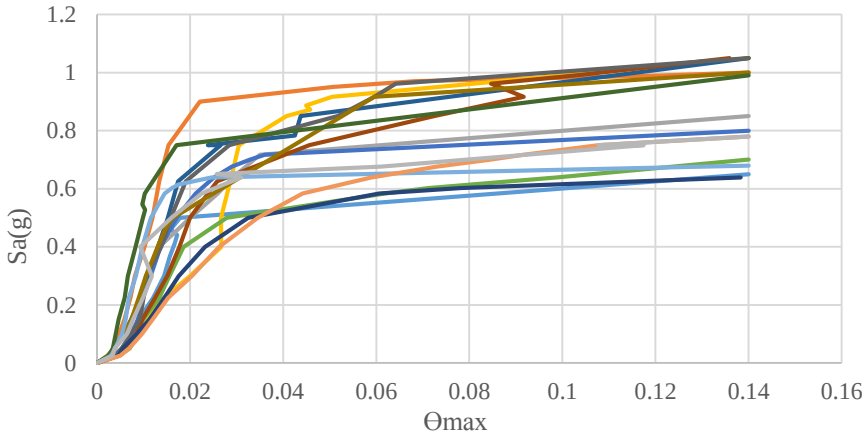

Figure 6. IDA analyses for 3-story building.

After the IDA was applied, fragility curves corresponding to collapse state has been obtained. The probability of each damage state is equal to the number of records entered to that damage state split up to total number of records. In Figure 7 fragility curves for each damage states of 3story-building with 5 second period isolators is presented. In order to make comparison easier, in the tables, the amount of median acceleration of collapse (Sa-50%) has been used. Since the structures that are compared have different periods, collapse margin ratio (CMR) is used. Finally Sa-50% collapse for far field and near field is compared.

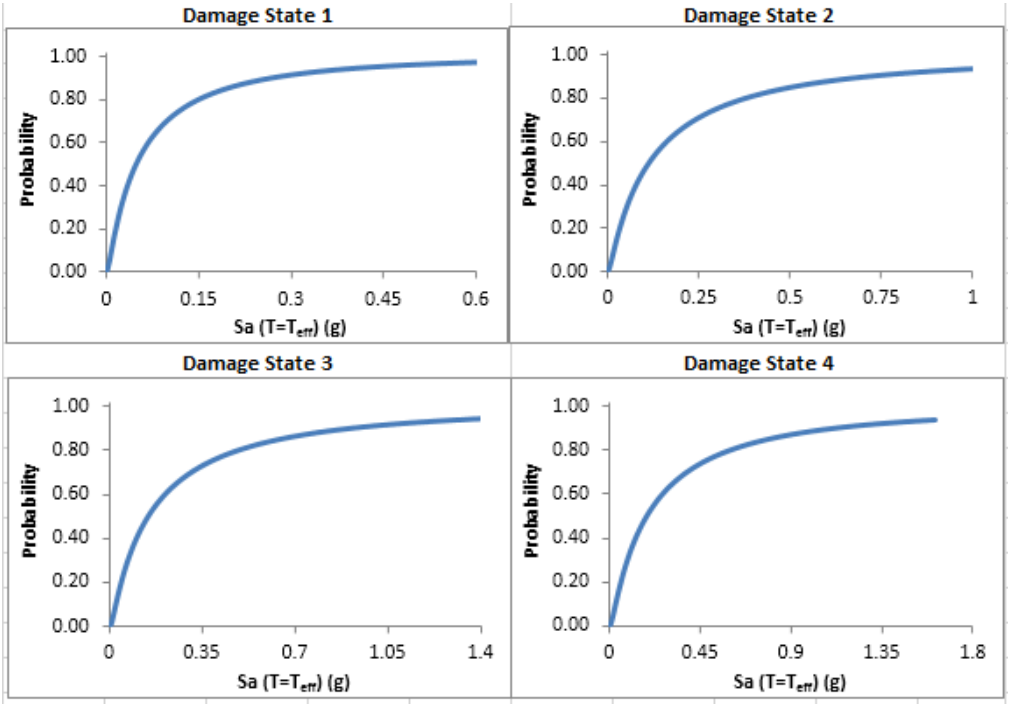

Figure 7. Damage states for 3-story building (T_{eff}=5sec).

6.2. Effect of isolator period

The isolation period is an important parameter in determination of fragility curves. So, in this section the collapse probability of base-isolated structures with different isolation period is considered and compared with Sa-50% and CMR.

6.2.1. Median acceleration collapse

Due to Figure 8 and the arrangement of fragility curves for three-story structures with different isolators subjected to far field earthquakes, it seems that the structure with lower period of isolator have better performance. In order to simplify the comparison, median acceleration of collapse (Sa-50%) for different isolators is presented in Table 2. According to Table 2 and Figure 8, by increasing the period of isolators Sa-50% collapse decreases. For example, 0.526, 0.312, and 0.183 belongs to Sa-50% of isolators with 3, 4, and 5 second period for 3-story building, respectively. This reduction can indicate the poor performance of isolators with higher periods moreover, as it is explained in section one, they must be compared with collapse margin ratio CMR to have a better comprehension of the effect.

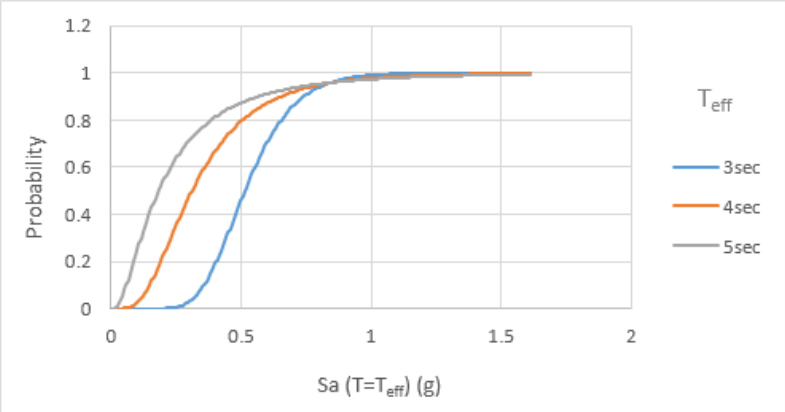

Figure 8. Fragility curves for 3-story building mounted on 3, 4, and 5 second period isolators subjected to far field earthquakes.

Table 2. 3-story building subjected to far field for collapse damage state

Period of isolator T_{eff} (sec)	Sa-50%collapse (g)
3	0.526
4	0.312
5	0.183

The effects of isolation period on the super-structure responses subjected to near field earthquakes are similar to far field ones. According to Table 3 and Figure 9 by increasing period of isolators, Sa-50% collapse decreases.

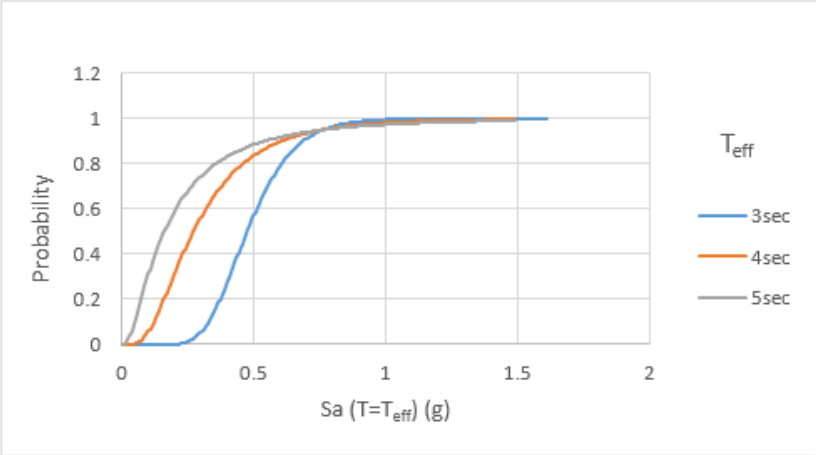

Figure 9. Fragility curves for 3-story building mounted on 3, 4, and 5 second period isolators subjected to near field earthquakes.

Table 3. 3-story building subjected to near field for collapse damage state.

Period of isolator T_{eff} (sec)	Sa-50%collapse (g)
3	0.496
4	0.273
5	0.162

6.2.2. CMR

As stated at the end of section 1, different period of isolators leads to different acceleration transitions to the isolated system. So, for better illustration of the effect of the isolation period, collapse margin ratio is obtained. The results are presented in Table 4. According to Table 4 the results indicate that isolators with higher periods, increases the CMR in the structure. That shows that an isolator with higher period has better performance and leads to a safer design. For instance, CMR for a three-story building with 3 and 5 second isolator period is 3.04 and 4.08 in the same order.

Table 4. Collapse margin ratio (CMR) for 3-story building subjected to far field and near field earthquakes.

	CMR	
T_{eff} (sec)	Far filed	Near field
3	3.04	2.87
4	3.74	3.27
5	4.08	3.62

6.3. Effect of far field and near field earthquakes

In this section, the effects of far field and near field earthquakes are presented for 3-story isolated building and the results are displayed in Table 5. Results illustrates that a structure subjected to near field earthquakes damages at a lower acceleration. For example, a three-story building mounted on 3 second period isolator have the median acceleration collapse of 0.496 and 0.526 for near field and far field earthquakes respectively, which demonstrates that better performance of isolator at far field earthquakes. Since in this comparison, the number of story and the effective periods of isolators are not variable, it is not necessary to compare them with collapse margin ratio.

Table 5. Sa-50% collapse for 3-story building.

	$Sa_{(collapse)}$-50% (g)	
T_{eff} (sec)	Far field	Near field
3	0.526	0.496
4	0.312	0.273
5	0.183	0.162

6.4. Effect of number of stories

In order to study the effect of number of stories, results of Sa-50% collapse for 3, 6, and 9 stories structures mounted on different periods of isolators are listed in Table 6 and 7. According to Table 6 and Figure 10, by increasing number of stories, Sa-50% collapse decreases. With a specific isolator and various floors, structure with more number of floors collapse at less Sa-50% collapse. For example, results of median acceleration collapse for 3 second period isolator in 3, 6, 9stories subjected to far field earthquakes are respectively 0.526, 0.356, and 0.274. According to Table 7 and Figure 11, the results of structures with different isolator and various number of floors subjected to near field earthquakes, show that Sa-50% collapse for one specific isolator decreases by increasing the number of floors. For example, results of median acceleration collapse for 3 second period isolator in 3, 6, 9stories subjected to near field earthquakes are respectively 0.496, 0.339, and 0.226.

Table 6. Structures subjected to far field earthquakes for collapse damage state.

Period of isolator T_{eff} (sec)	3-strory	6-story	9-story
3	0.526	0.356	0.274
4	0.312	0.296	0.254
5	0.183	0.164	0.149

Table 7. Structures subjected to near field earthquakes for collapse damage state.

Period of isolator T_{eff} (sec)	3-strory	6-story	9story
3	0.496	0.339	0.226
4	0.273	0.25	0.154
5	0.162	0.154	0.135

Advance Researches in Civil Engineering
ISSN: 2645-7229, Vol.4, No.4, pages: 1-15

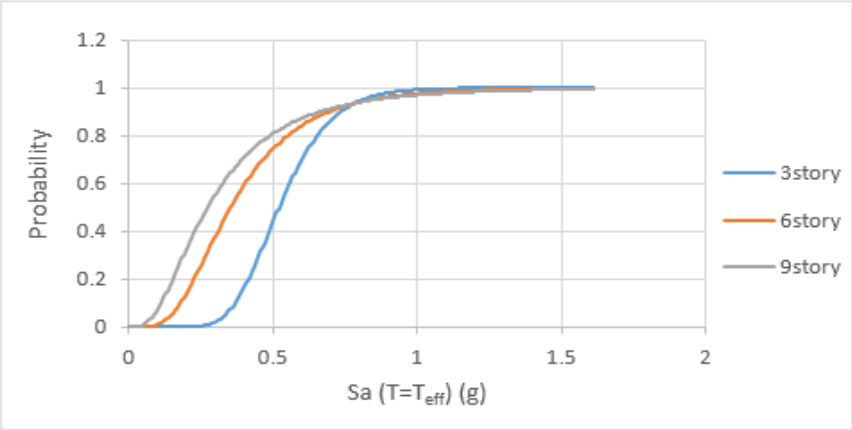

Figure 10 Fragility curves for 3, 6 and 9 story building mounted on 3second period isolator subjected to far field earthquakes.

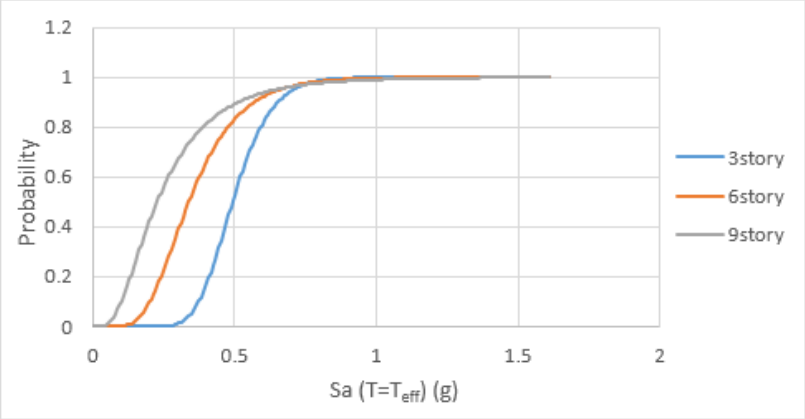

Figure 11. Fragility curves for 3, 6 and 9 story building mounted on 3second period isolator subjected to near field earthquakes.

7. Conclusions

Over the past two decades with advances in technology and construction methods, new facilities have been introduced to reduce impacts of earthquakes on structures. Base-isolations as an efficient method, along with usual solutions, has always been remarkable for engineers and designers. One of the most important type of isolators, is friction isolator. Among the types of frictional isolators, triple concave friction pendulum (TCFP) is the newest one. Although researches has been done on TCFP structural performance, but many points in dynamic and seismic behavior have not been fully determined. In this paper, the seismic performance of TCFP base-isolated structure is considered to obtain generally behavior of TCFP isolators. For this purpose, 3, 6, and 9 stories structures mounted on TCFP isolators with different isolation periods (3, 4, and 5 seconds) are assumed. Fragility curves for each model in collapse state are calculated based on IDA analyses. And they are subjected to 15 near field and 15 far field earthquakes and the results are compared. By increasing the period of isolators Sa-50% collapse decreases. For example 0.526, o.312, and 0.183 belongs to Sa-50% of isolators with 3 second, 4, and 5 second period for three-story

structures. Concept of collapse margin ratio indicates the structural safety in collapse state. By comparing CMRs for different structures, it is concluded that structures with higher isolator periods have a better performance and has more safety. For example for three-story structure CMR of a 3 second period isolator is 3.04 and for 5 second isolator is 4.08. Comparing a specific structure subjected to far field and near field earthquakes demonstrates that structure subjected to near field earthquakes damages at a lower acceleration. For instance, three-story structure mounted on 3 second period isolator owns the median acceleration collapse of 0.496 for near field and 0.526 for far field earthquakes which demonstrates a better performance of isolator at far field earthquakes. Comparing Sa-50% collapse for specific isolator and various number of stories indicates that Sa-50% collapse for one specific isolator decreases by increasing the number of stories.

8. References

1- Zayas, V., Low, S., Bozzo, L. and Mahin S.A., 1989, **Feasibility and performance studies on improve the earthquake resistance of new and existing building using the Friction Pendulum system**, Report No.UCB/EERC-89/09, Earthquake Research Center, University of Berkeley.

2- Tsopelas, P., Constantinou, M.C., Kim Y. S. and Okamoto S., 1996, **Experimental Study of FPS System in Bridge Seismic Isolation**, Earthquake Engineering and Structural Dynamics, 25, 65-78.

3- Khoshnoudian, F. and Rabie, M. 2011, **Response of Multistory Friction Pendulum Base-isolated Buildings including the Vertical Component of Earthquakes**, Canadian journal of Civil Engineering, 38(10), 1045–1059.

4- Castaldo, P., Mancini, G. and Palazzo, B., 2018, **Seismic reliability-based robustness assessment of three-dimensional reinforced concrete systems equipped with single-concave sliding devices**, Engineering Structures, 163, 373-387.

5- Tsai, C.S., Chen, B.J., Pong, WS. and Chiang, TC., 2004, **Interactive Behavior of Structures with Multiple Friction Pendulum Isolation System and Unbounded Foundations**, Advances in Structural Engineering, 7, 539–551.

6- Fenz, D. and Constantinou, M.C. 2006, **Behavior of the double concave friction pendulum bearing**, Earthquake Engineering and Structural Dynamics, 35, 1403–1424.

7- Rabie, M. and Khoshnoudian, F., 2013, **Seismic response of elevated liquid storage tanks using double concave friction pendulum bearings with tri-linear behavior**, Advances in structural engineering, 16, 315–338.

8- Khoshnoudian, F. and Hemmati, A., 2013, **Impact of structures with double concave friction pendulum bearings on adjacent structures**, Proceedings of the Institution of Civil Engineers Structures and buildings, 167, 41–53.

9- Zhou, F., Xiang, W., Ye, K. and Zhu, H., 2019, **Theoretical study of the double concave friction pendulum system under variable vertical loading**, Advances in structural engineering, 22(8), 1998-2005.

10- Fenz, D. and Constantinou, M. C., 2008, **Modeling Triple Friction Pendulum Bearings for Response History Analysis**, Earthquake Spectra, 24(4), 1011-1028.

11- Fadi, F. and Constantinou, M. C., 2009, **Evaluation of Simplified Methods for Analysis for structures with Triple Friction Pendulum isolators**, Earthquake Engineering and Structural Dynamics, 39, 5-22.

12- Morgan, T.A. and Mahin, S. A., 2011, **The Use of Base Isolation Systems to Achieve Complex Seismic Performance Objectives**, Technical Report PEER 2011/06, Pacific Earthquake Engineering Research Center, University of California, Berkeley, CA, USA.
13- Becker, T.C. and Mahin, S. A., 2012, **Experimental and Analytical study of the Bi-directional Behavior of the Triple Friction Pendulum Isolator**, Earthquake Engineering and Structural Dynamics, 41, 355-373.
14- Loghman, V. and Khoshnoudian, F., 2015, **Comparison of Seismic Behavior of Long Period SDOF Systems Mounted on Friction Isolators under Near-Field Earthquakes**, Smart Structures and Systems, 14(4), 1-23.
15-Loghman, V.,Tajammolian, H. and Khoshnoudian, F., 2015a, **Effects of rotational components of earthquakes on seismic responses of triple concave friction pendulum base-isolated structures**, Journal of Vibration and Control, 23, 1495-1517.
16- Loghman, V., Khosnoudian, F. and Banazadeh, M., 2015b, **Effects of vertical component of earthquake on seismic responses of triple concave friction pendulum base-isolated structures**, Journal of Vibration and Control, 21, 2099-2113.
17- Fallahian, M., Khoshnoudian, F. and Loghman, V., 2015, **Torsionally Seismic Behavior of Triple Concave Friction Pendulum Bearing**, Advances in Structural Engineering, 18(12), 2151-2166.
18- Tajammolian, H., Khoshnoudian, F and Partovi Mehr, N., 2016, **Seismic Responses of Isolated Structures with Mass Asymmetry Mounted on TCFP Subjected to Near-Fault Ground Motions**, International Journal of Civil Engineering, 14, 573-584.
19- Becker, T.C., Bao, Y. and Mahin, S. A., 2017, **Extreme behavior in a triple friction pendulum isolated frame**, Earthquake Engineering and Structural Dynamics, 46(15), 2683-2698.
20- Xu, Y., Guo, T. and Yan, P., 2019, **Design optimization of triple friction pendulums for base-isolated high-rise buildings**, Advances in Structural Engineering, 22(13), 2727-2740.
21- Dao, N.D., Ryan, K.L. and Nguyen-Van, H., 2019, **Evaluating simplified models in predicting global seismic responses of a shake table-test building isolated by triple friction pendulum bearings**, Earthquake Engineering and Structural Dynamics, 48(6), 594-610.
22- HAZUS, 2003, **HAZUS-MH 2.1Advance Engineering Building Module, Technical and User's Manual**, Federal Emergency Management Agency, Department of Homeland Security Emergency Mitigation Division.
23- Constantinou, M. C, Kalpakidis, I., Filiatrault, A. and Ecker Lay, R. A., 2011, **LRFD-Based Analysis and Design Procedures for Bridge Bearings and Seismic Isolation**, Technical Report No. MCEER-11-0004, New York, Buffalo.
24- Fenz, D. and Constantinou, M. C., 2008, **Mechanical Behavior of Multi-Spherical Sliding Bearings**, Report No. MCEER-08/0007, New York, Buffalo: MCEER.
25- Federal Emergency Management Agency, 1997, **Quantification of Building Seismic Performance Factor (FEMA-P695)**, Applied Technology Council.
26- Vamvatsikos, D. and Cornell, CA., 2003, **Incremental dynamic analysis**, Earthquake Engineering and Structural Dynamics, 31, 491–514.
27- Zhang, J. and Huo, Y., 2009, **Evaluating effectiveness and optimum design of isolation devices for highway bridges using the fragility function method**, Engineering Structure, 31, 1648–1660 (2009).
28- Tavares, D. H., Suescun, J. R., Paulter, P., and Padgett, J. E., 2013, **Seismic Fragility of a Highway Bridge in Quebec**, Journal of Bridge Engineering, 18(11), 1131-1139.

29- Han, R., Li, Y. and Van de Lindt, J., 2014, **Seismic risk of base isolated non-ductile reinforced concrete buildings considering uncertainties and mainshock–aftershock sequences**, Structural Safety, 50, 39-56.
30- Zhou,C. Zeng, X. Pan, Q. and Liu, B., 2014, **Seismic fragility assessment of a tall reinforced concrete chimney**, Structure Design Tall Special Buildings, 24(6), 440-460.
31- Phan, HN., Paolacci, F., Uckan, C, and Shen, J. J., 2016, **Seismic vulnerability mitigation of liquefied gas tanks using concave sliding bearings**, Bulletin of Earthquake Engineering, 14, 3283–3299.
32- Castaldo, P., Amendola, G. and Palazzo, B., 2017, **Seismic fragility and reliability of structures isolated by friction pendulum devices: seismic reliability-based design (SRBD)**, Earthquake Engineering and Structural Dynamics, 46, 425-446.
33- Castaldo, P., Amendola, G. and Ripani, M., 2018, **Seismic fragility of structures isolated by single concave sliding devices for different soil conditions**, Earthquake Engineering and engineering vibration, 17, 869-891.
34- ASCE7-10, 2010, **Minimum Design Loads for Building and Other Structures**, Published by American Society of Civil Engineers. Virginia, USA.
35- AISC 360-10, 2010, **Specification for Structural Steel Buildings**, Published by American Institute of Steel Construction. Chicago, Illinois, USA.
36- AISC 341-10, 2010, **Seismic provisions for structural steel buildings**, Published by American Institute of Steel Construction. Chicago, Illinois, USA.
37- PEER. Open System for Earthquake Engineering Simulation (OpenSees) development platform by the Pacific Earthquake Engineering Research Center (PEER). http://opensees.berkeley.edu. (2008).
38- Mazzoni, S., McKenna, F., Scott, M. H, and Fenves, G. L., 2007, **OpenSees command language manual**, Pacific Earthquake Engineering Research Center, 451.